J. Fluid Mech. (2006), *vol.* 566, *pp.* 97–115.
doi:10.1017/S0022112006002473 Printed in the United Kingdom

Relaminarization in highly favourable pressure gradients on a convex surface

By R. MUKUND[1], P. R. VISWANATH[1], R. NARASIMHA[2], A. PRABHU[3] AND J. D. CROUCH[4]

[1]Experimental Aerodynamics Division, National Aerospace Laboratories, Bangalore 560 017, India

[2]Engineering Mechanics Unit, Jawaharlal Nehru Centre for Advanced Scientific Research, Jakkur, Bangalore 560 064

[3]Aerospace Engineering Department, Indian Institute of Science, Bangalore 560 012

[4]Boeing Commercial Airplanes, Seattle, WA 98124, USA

(Received 4 March 2006 and in revised form 4 April 2006)

We report here the results of experiments on two flows – one on a convex surface and the other on a flat surface – designed to bring out explicitly the influence of streamwise curvature on relaminarization in highly favourable pressure gradients. In both flows, the initial conditions and the streamwise distribution of the Launder pressure-gradient parameter K are virtually identical. The maximum value of K is 6.2×10^{-6}, well above the critical value of about 3.5×10^{-6} usually advocated for relaminarization. The spatial extent of the acceleration zone is of order 10 initial boundary-layer thicknesses, appreciably shorter than in earlier work in order better to simulate conditions at the leading edge of a typical aircraft wing. The fall in skin friction coefficient is steeper and the rise in shape factor sharper on the convex surface than on the flat surface, indicating that relaminarization on the convex surface is both more rapid and more nearly complete. In the crucial relaminarizing zone, two-layer quasi-laminar theory is found to predict the convex-surface mean-flow parameters more accurately than the flat-surface flow, without any explicit modelling of curvature effects. Thus, experimental results and supporting calculations both indicate that the dominant effect of streamwise convex curvature on the mean flow is to promote more rapid and complete relaminarization in an accelerated turbulent boundary layer, thus enhancing the probability of its occurrence on the leading edge of swept wings where both factors are significantly in operation.

1. Introduction

Interest in relaminarization of strongly accelerated turbulent boundary layers has been revived by the recognition that it may routinely occur in the leading-edge region of swept wings at high lift (Van Dam *et al.* 1993 and Arnal & Juillen 1990; Thompson 1972 appears to have been the first to suggest such a possibility). The attachment-line boundary layer of a swept wing becomes turbulent at sufficiently high Reynolds numbers, resulting in partial loss of lift due to thicker boundary layers at the trailing edge. However, the attachment line shifts to the pressure surface at high incidence, and the streamwise boundary layer passing over the wing leading edge experiences strong acceleration. This may result in relaminarization, leading to some recovery in the maximum lift (Yip *et al.* 1996). Such a boundary layer encounters not only high acceleration but also high convex curvature, and the relative significance of these

Reference	Code	U_0 (m s^{-1})	$R_{\theta 0}$	$K_{\max} \times 10^6$	x_a/δ_0
Brandt (1993)	A1	8	373	10.5	66
	A2	12	559	7.1	57
	A3	16	730	5.5	57
	A4	20	839	4.9	56
	B1	8	280	4.3	65
	B2	12	482	3.3	50
Warnack & Fernholz (1998)	WF2*	7.77	862	4.0	27
	WF4*	7.79	2564	3.9	20
Escudier *et al.* (1998)		4	1700	4.4	23
Ichimiya *et al.* (1998)		6	799	6	32
Bourassa *et al.* (2000)		4	1545	4.10	

* Axisymmetric flow.

TABLE 1. Recent experiments on relaminarization due to high acceleration.

effects has never been established. Meanwhile, the empirical relationships used to predict the occurrence of relaminarization take no account of the potential role of surface curvature, such relationships being based on two-dimensional flat-plate experiments.

A complete understanding of relaminarization phenomena relevant to swept wings would involve consideration of transition to turbulence by different mechanisms preceding and following relaminarization (a preliminary account of some relevant experiments is given by Viswanath *et al.* 2004), and a consideration of flow three-dimensionality. Furthermore, flow measurements inside the thin boundary layers present in the leading-edge region of a swept wing are rather difficult. We have therefore undertaken some building-block experiments in two-dimensional flow, systematically investigating the combined effects of pressure gradient and convex curvature on an originally turbulent boundary layer.

The early experimental studies on flat-plate boundary-layer relaminarization were reviewed by Narasimha & Sreenivasan (1973, hereafter referred to as NS73; 1979) and Sreenivasan (1974, 1982). These and some more recent experiments (Brandt 1993; Escudier *et al.* 1998; Ichimiya, Nakamura & Yamashita 1998; Warnack & Fernholz 1998; Bourassa, Thomas & Nelson 2000; Kobashi & Hayakava 2002 – catalogued in table 1 for reference) show that the whole flow can be conveniently divided into four distinct zones. In the first zone, where the pressure gradient is still relatively low, a classical fully there is turbulent boundary layer subjected to a (mild) favourable pressure gradient, displaying the expected slight rise in skin friction and fall in shape factor. In the second, relaminarizing zone, the law of the wall breaks down, the boundary layer becomes thinner, and eventually the shape factor increases and the skin friction coefficient C_f decreases towards laminar values. This relaminarization is a relatively rapid process in which an initially turbulent boundary layer can be rendered effectively laminar over distances of 20–30 boundary layer thicknesses or less. Velocity fluctuations may still remain in the relaminarized state, but their contribution to mean flow dynamics is small, in particular because the Reynolds shear stresses tend to freeze (Narasimha & Sreenivasan 1979). However, the residual disturbances present in the flow promote rapid retransition of the relaminarized boundary layer soon after the favourable pressure gradient is relieved; this constitutes the third zone. Finally, in the fourth zone, the flow returns to a standard fully turbulent state.

Various authors have proposed different parameters as criteria for marker events in the process of relaminarization. The acceleration parameter $K = \nu U_e^{-2} \mathrm{d}U_e/\mathrm{d}x$ of Launder (1964) is a simple free-stream parameter that is widely used as an indicator of the onset of relaminarization; here U is the velocity at the edge of the boundary layer, x is streamwise coordinate and ν the kinematic viscosity of the fluid. This and other criteria are reviewed in NS73. Narasimha & Sreenivasan (1979, see e.g. pp. 250, 251) suggested that a parameter equivalent to KC_f^{-n} (where C_f is the skin friction coefficient and $n = 3/2$ according to many workers) locates the onset of relaminarization, but, to the extent that C_f varies only slowly with Reynolds number in turbulent flow, K can itself be useful in that role at modest Reynolds numbers. In contrast, the completion of relaminarization can be defined with considerable confidence, with the aid of a theory that views relaminarization as an asymptotic process involving a large value of the ratio (denoted by Λ) of the streamwise pressure gradient to the characteristic Reynolds-stress gradient across the flow. For large values of Λ a two-layer treatment, involving what were called the quasi-laminar equations (QLE), was developed for predicting the mean flow parameters during the crucial relaminarizing process (zone two). The initial near-wall part of this zone, which could neither be computed by turbulent boundary layer calculations nor by QLE, was termed the 'island of ignorance' by NS73. The value of the theory was demonstrated by the successful prediction of a variety of boundary-layer parameters in the relaminarizing zone. On similar lines, Brandt (1993) proposed the parameter $K^* = \nu U_{e0}^{-2}\ \mathrm{d}U_e/\mathrm{d}x$ (where U_{e0} is the free-stream velocity ahead of acceleration) and found that K^* exceeded 8.1×10^{-6} in the relaminarizing flows he investigated.

Experiments on boundary-layer flows over surfaces with streamwise curvature reveal that convex curvature inhibits turbulence and has a first-order stabilizing effect on a turbulent boundary layer (e.g. Bradshaw 1973; Patel & Sotiropoulus 1997). This is more significant than the second-order effect found in laminar boundary layers (Narasimha & Ojha 1967). Curvature effects are generally characterized by the parameter $k\delta$ or $k\delta_0$, where $1/k$ is the radius of curvature and δ is the boundary layer thickness, δ_0 being its value at the start of curvature.

The major effects of the convex curvature on a turbulent boundary layer are as follows. First, it decreases the extent of the logarithmic region and the value of the intercept in the log law (for $k\delta > 0.03$, Prabhu, Narasimha & Rao 1983). Secondly, the growth of boundary-layer thickness is lower than that on a flat surface for small $k\delta$ (Gibson, Verriopoulos & Vlachos 1984), becoming negligible for high $k\delta$ (So & Mellor 1973; Prabhu & Sundarasiva Rao 1981), thereby reducing the entrainment as well. The skin friction coefficient decreases with increasing Reynolds number (based on the boundary-layer thickness) more rapidly than on a flat surface, while the shape factor increases, both having a strong dependence on $k\delta$. A collapse of velocity profiles in outer coordinates centred on the position of maximum velocity has also been observed (Prabhu *et al.* 1983), indicating that the outer flow is effectively stress-free and vorticity is conserved along streamlines. All these effects are reminiscent of those experienced with high acceleration. The experiments of So & Mellor (1973) have further shown that all three components of turbulence intensity and the shear stress reduce dramatically in the outer region, with the correlation coefficient associated with the latter vanishing or even changing sign for $y/\delta > 0.4$. It is therefore clear that convex curvature will promote relaminarization.

There have been only two earlier studies on the combined effects of convex surface curvature and favourable pressure gradients. Launder & Loizou (1992) conducted experiments in a rectangular-sectioned bend having a converging sidewall, but their

Flow	Surface	U_0 (m s^{-1})	$R_{\theta 0}$	$K_{\max} \times 10^6$	δ_0 (mm)	x_a/δ_0	δ_0/R_w	$\Lambda_{\max}$
CP1	Convex	11.3	1710	6.2	26.5	10	0.0275	158
FP1	Flat	11.72	1670	6.2	24.1	12	–	159
CP2	Convex	15.3	2000	9.0	26.5	7	0.0275	325

TABLE 2. Experimental conditions for the three flows.

measurements were hampered by the secondary flow present in the duct. Schwarz & Plesniak (1996) made LDV measurements in turbulent boundary layers on a convex surface with $k\delta_0 = 0.1$, subjected to relatively small favourable pressure gradients ($K_{\max} = 0.55 \times 10^{-6}$, 1.01×10^{-6}). Although the Reynolds stress on the convex-surface flow decreased considerably in the outer region of the boundary layer, the flow did not relaminarize. No studies have been made to-date on curved surfaces with the higher favourable gradients associated with relaminarization.

This paper considers the effects of convex surface curvature in promoting relaminarization of an accelerated turbulent boundary layer in a two-dimensional flow. The experimental flow conditions are tuned to be relevant to relaminarization occurring on swept-wing leading edges under high-lift conditions.

2. Experimental set-up

Experiments were conducted on two key configurations having virtually identical initial conditions and K distributions. (From the discussion in the previous section, this will amount to having nearly identical distributions of parameters like KC_f^{-n}; in what follows we will mention only K, which, being a purely free-stream parameter, is a useful measure of the pressure gradient for the purposes of the present investigations.) One of the configurations had a convex curved surface, the other being flat; these configurations are designated CP1 and FP1 respectively. Selected results from an additional convex surface experiment CP2 will be used to supplement the data on CP1. Table 2 gives a comparison of these flows. These experiments differ from earlier work on two-dimensional relaminarizing flows in the following major respects: (i) the simultaneous presence of strong acceleration and streamwise convex curvature, (ii) a significantly shorter extent of acceleration, and (iii) a region of mild adverse pressure gradient at the end of the acceleration affecting the retransition process. As we shall see, both flows CP1 and FP1 have virtually the same acceleration distribution. In addition, the non-dimensional pressure gradient $(\delta/\rho U^2)\,\mathrm{d}p/\mathrm{d}x$ and the curvature parameter $k\delta$ have been chosen to provide conditions similar to those occurring on swept wings at flight Reynolds numbers scaled on boundary-layer thickness.

The experiments were conducted in the 1.5 m low-speed wind tunnel at the Experimental Aerodynamics Division of National Aerospace Laboratories, Bangalore. The model configuration (figure 1) used for the convex-surface experiments consisted of a leading-edge region followed by a stretch of flat plate and a convex aft section. The whole model was placed between two sidewall inserts 0.6 m apart. A strip of emery paper pasted at $x = 0.24$ m on the flat plate acted as a boundary layer trip and provided a thick and reasonably well-developed turbulent boundary layer growing at constant pressure till the end of the flat section. The required favourable pressure gradients were imposed on the surface by locating a pressure-generator airfoil close to it (figure 1). In order to achieve the desired pressure distributions specific airfoils were

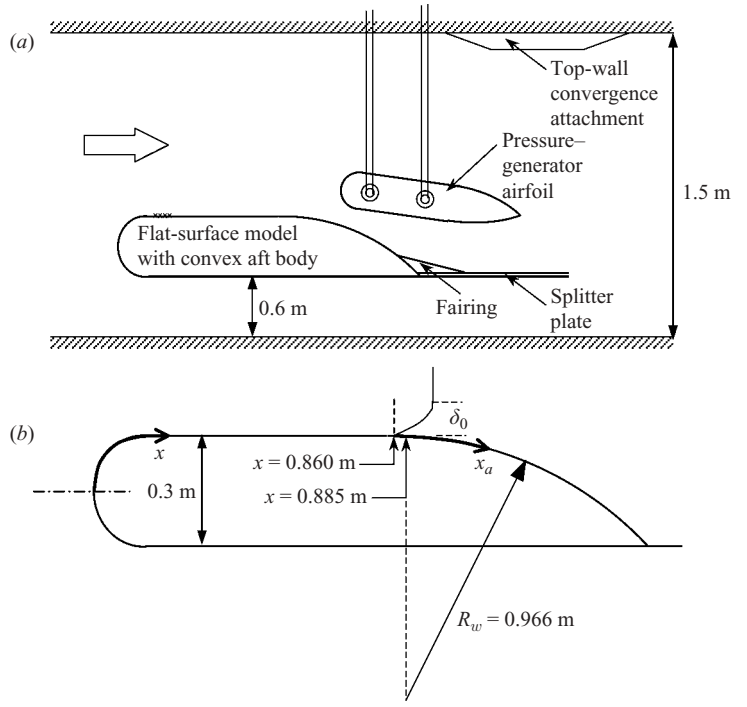

FIGURE 1. The model layout for the convex-surface experiments. (*a*) Sketch of the model layout in the 1.5 m wind tunnel. (*b*) Sketch of the model indicating some dimensions and definitions.

designed for each flow, using a panel code. The location and incidence of the airfoil provided just enough control to obtain, with a combination of extensive panel code computations and some experimental fine tuning, virtually identical K-distributions in both CP1 and FP1 (as we shall see below). Further details of the set-up are presented in Mukund (2002*a*).

The test surface (figure 1*a*) was provided with 48 static pressure ports (0.7 mm inner diameter) located typically 20 mm apart along the centreline, connected to scanivalves coupled to micro-manometers (Furness Control, UK). The boundary-layer mean velocity and streamwise turbulent intensity profiles were measured at several streamwise locations on the test surface using a single hot wire (2.5 mm long 5 μm diameter tungsten) connected to a DISA 55M01 constant-temperature anemometer (CTA). The mean and fluctuating wall shear stress were measured using hot-film gauges (No. WTG-50, Micro Measurements, USA), having a cold resistance of 50 ohms, connected to the CTA. In order to overcome the difficulties encountered in the *in-situ* calibration of the hot-film gauges on the convex surface, they were bonded on top of cylindrical Teflon plugs and calibrated in the zero-pressure-gradient flat-surface boundary layer upstream ($x = 0.86$ m), the reference shear stress being obtained from Pitot profiles using Clauser plots. The gauges were moved to different locations on the convex surface for measurement. This method had the advantage that wall stress measurements at all the selected locations could be carried out with a single calibrated gauge. (Wall shear stress values ranged from 2.3 to 10.9 Pa in the measurements, well within the calibration range of 2 to 17 Pa.) The use of plugs having a flat top was feasible on the convex test surface since the radius of curvature

Index	x_a (m)	$K \times 10^6$	$k\delta$ (CP1)
A	0.000	0.4	0.026
B	0.165	4.2	0.023
C	0.225	4.8	0.019
D	0.265	1.8	0.017
E	0.285	0.4	0.015
F	0.305	−0.8	0.013
G	0.325	−1.6	0.012
H	0.345	−2.1	0.012
I	0.385	−2.2	0.016

Note : $x_a = x - 0.860$ for CP1, $= x - 0.890$ for FP1.

TABLE 3. Common hot-wire measurement locations for FP1 and CP1.

was large (966 mm) compared to the plug diameter (14 mm). In order to use a hot-film gauge possessing a common calibration for both laminar and turbulent boundary layers, it is necessary that the thermal boundary layer formed by the heated gauge be well within the viscous sublayer (Liepmann & Skinner 1954). Experiments conducted in both laminar and turbulent flows showed that a common calibration is valid up to an overheat ratio of 1.20 and hence this value was chosen for this experiment.

All the mean velocity data were acquired digitally and averaged over 10 s. The instantaneous signals from hot-wire and hot-film probes were acquired at a rate of 4 kHz and 2 kHz respectively for 15 s. The flow two-dimensionality was assessed to be satisfactory by three methods, namely, oil flow visualization, spanwise invariance of static pressure, and consistency of measured momentum thickness with the two-dimensional momentum integral balance (Mukund 2002*a*). Measurement uncertainties were estimated using data from instrument manufacturers, laboratory calibration and repeatability tests. Using the method suggested by Kline & McClintock (1953), the overall uncertainty in the pressure coefficient C_p, mean velocity u, velocity fluctuations u' and the skin friction coefficient C_f are estimated to be less than 2 %, 2.5 %, 4 % and 8 % of the maximum values respectively.

3. Results

Comparison of the distribution of K in flows FP1 and CP1 (figure 2*a*) shows an excellent match, thus enabling direct assessment of the effect of curvature. (The abscissa in figure 2 is x_a, measured from an effective origin at station A at which the pressure gradient is very small, $K = 0.4 \times 10^{-6}$. Note that the coordinate x is measured along the surface, from the leading edge for the flat plate and from the front stagnation point for the curved surface.) The value of $K_{\max}$ in both flows is 6.2×10^{-6}, well above the usually quoted critical value of 3.5×10^{-6}. Figure 2(*c*) shows the parameter $k\delta$ for CP1, and figure 2(*b*) the selected stations (designated A to I) along the surface at which common measurements were made. Table 3 lists the designated common locations.

3.1. *Mean velocity profiles*

The mean streamwise velocity profiles in the boundary layer for both CP1 and FP1 are shown in figures 3 and 4 in terms of outer and wall coordinates respectively. (The friction velocity u^* used in figure 4 has been consistently derived from interpolated

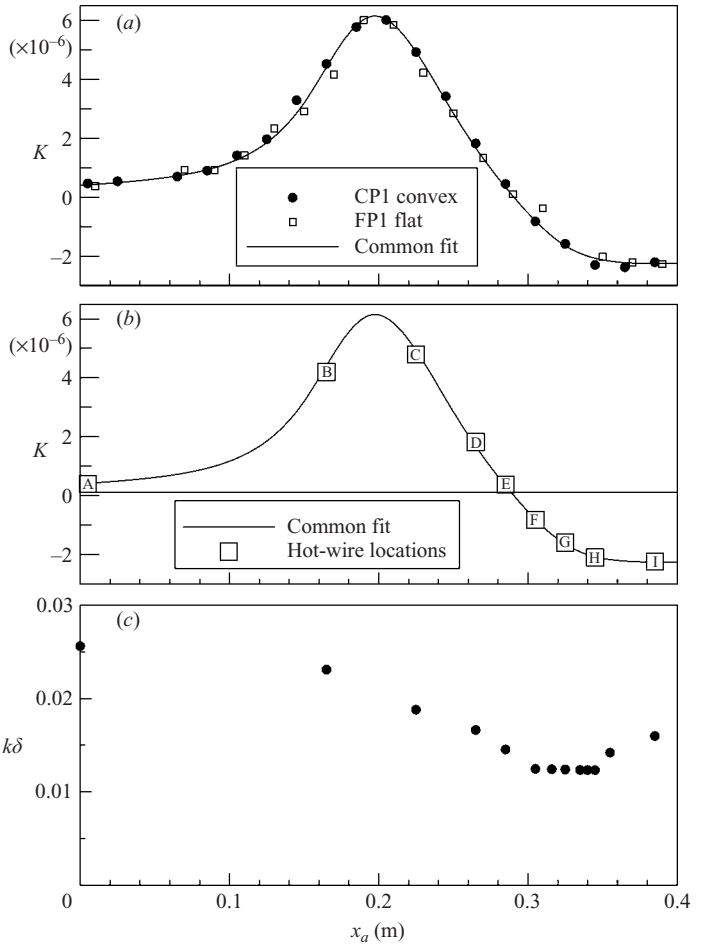

FIGURE 2. (*a*) The distribution of the acceleration parameter K comparing FP1 and CP1. (*b*) The hot-wire locations. (*c*) Parameter $k\delta$ for CP1.

values of the measured hot-film skin friction data.) Although the gradient $\partial u/\partial y$ is expected to be negative away from the boundary layer over a convex surface, the presence of the pressure-generator airfoil with its own convex surface in close proximity acts to counter this effect. Thus $\partial u/\partial y$ just beyond the edge of the boundary layer in CP1 is so weak as to be virtually indistinguishable from the data for FP1. The inviscid potential velocity $U_p(y)$ can be therefore taken to change little across the boundary layer, and consequently can be approximated by the edge velocity $U_e(x)$. It has been shown in Mukund (2002*a*) that the integral thickness parameters are negligibly different from those calculated using the extrapolation of $U_p(y)$ to $y=0$; in any case, these procedures have little effect on the calculated boundary layer parameters or on the conclusions drawn.

From figure 3, we see (as expected) that at station A there is hardly any difference between FP1 and CP1. Further downstream the profiles are typical of accelerated turbulent boundary layers, involving a large reduction in δ, accompanied by a fuller velocity profile close to the wall. At C, just past $K_{\max}$, and at D the differences between CP1 and FP1 are appreciable, indicating that curvature is exerting a strong

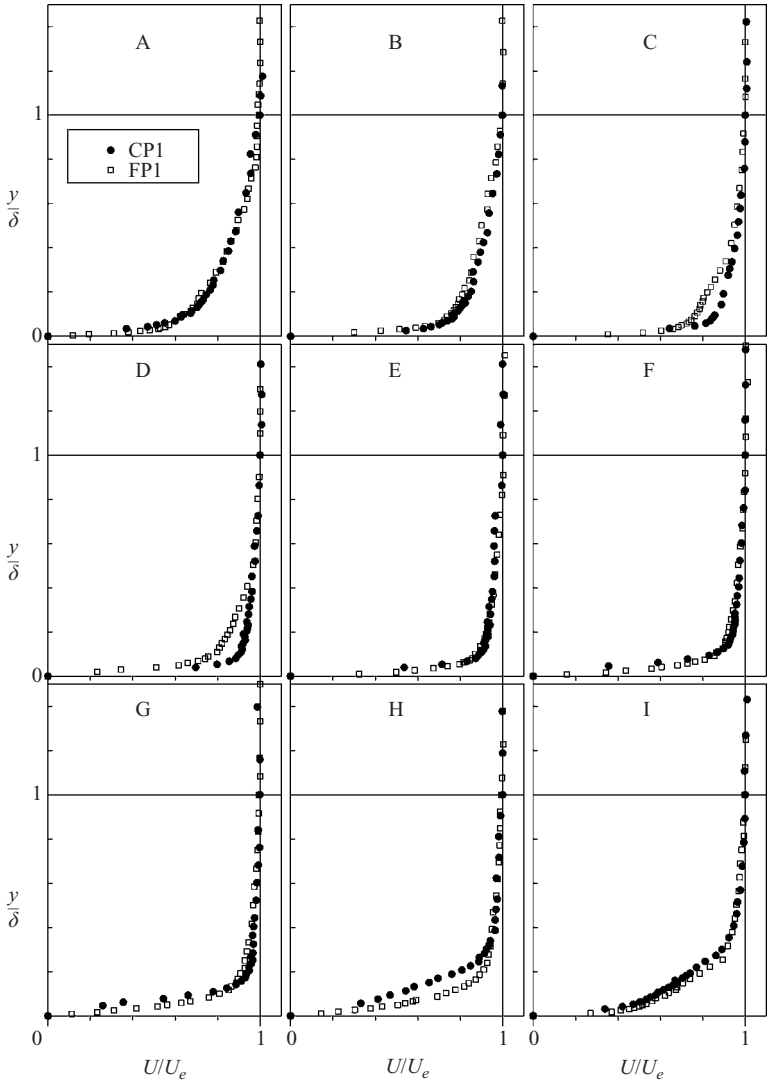

FIGURE 3. Mean velocity profiles in outer coordinates comparing the convex-surface flow CP1 and flat-surface flow FP1. For details of the parameters or A–I see table 3.

influence on the dynamics through the reduction of the Reynolds shear stress. At E both pressure gradient and the curvature parameter ($k\delta$, figure 2*c*) have fallen, and the CP1 and FP1 profiles are close to each other. In the beginning of the adverse-pressure gradient region δ remains nearly constant (figure 2*c*), and the profiles exhibit some degree of retardation near the wall, but further downstream δ increases. At stations H and I the adverse pressure gradient increases, and the difference between CP1 and FP1 at H is due to the earlier retransition in the former, as we shall discuss below.

The mean streamwise velocity profiles in wall coordinates comparing FP1 and CP1 are shown in figure 4. It is seen that the thickness of the outer (wake) layer diminishes in the favourable-pressure-gradient region, and eventually the outer velocity profile goes below the reference flat-plate logarithmic line (for CP1 at station C). Such a

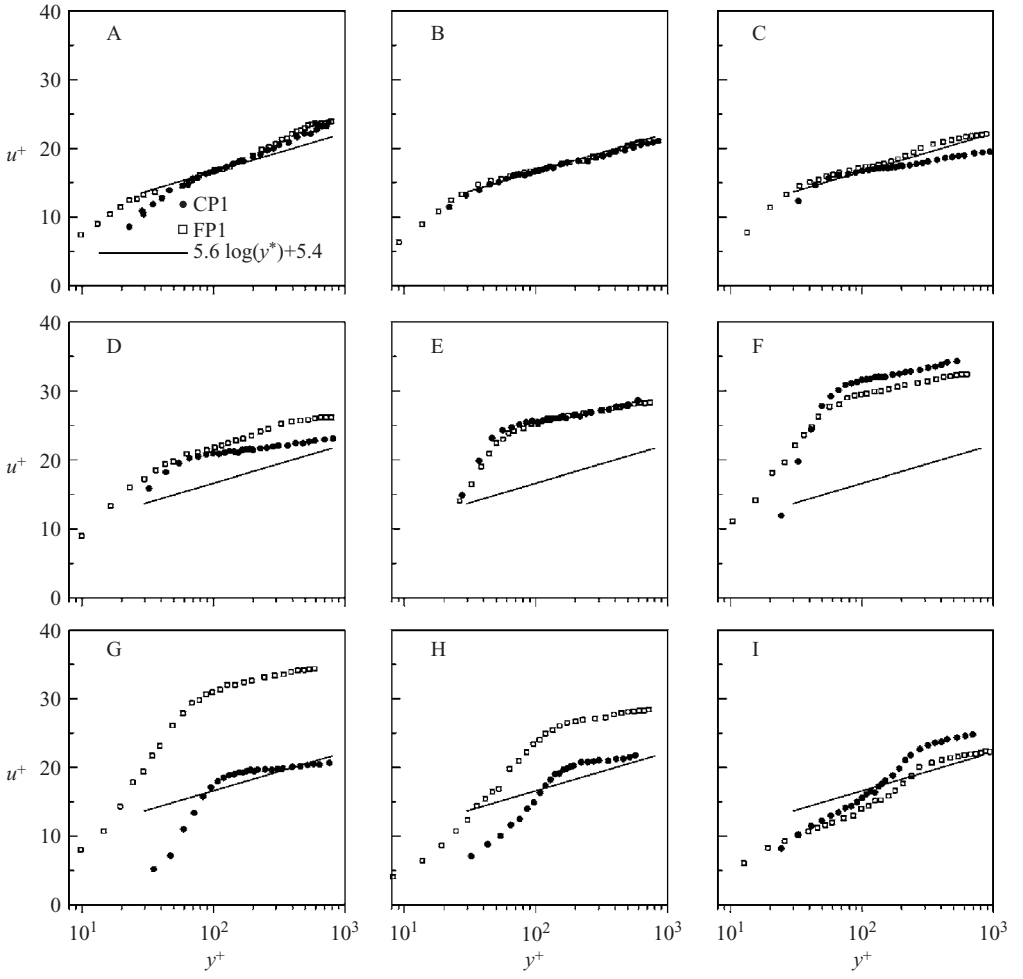

FIGURE 4. Mean velocity profiles in wall coordinates, comparing CP1 and FP1.

trend is typical of accelerated turbulent boundary layers (Badri Narayanan & Ramjee 1969; Blackwelder & Kovasznay 1972). The virtual disappearance of the law of the wall beginning near C is already an indicator of the onset of relaminarization. Further downstream at stations D, E and F there is a progressive upward shift of the profiles on the ordinate ($u^+ = u/u^*$), as C_f is dropping relatively faster in the present flows (to be discussed in §4). Further downstream, at stations G and H, the profiles shift downwards on the u^+ scale towards the reference log line, consistent with the C_f increase caused by the retransition of the relaminarized boundary layer in the weak adverse pressure gradient (§4). The profile at station I shows a tendency to redevelop a logarithmic region.

As far as the differences between CP1 and FP1 are concerned, the wall-law profiles in Figure 4 show the same trend at stations A to F as in figure 3. The largest deviations from the standard log law occur at stations F and G. At F, the difference between CP1 and FP1 is small suggesting that the profiles represent the responses of a relaminarized boundary layer to an adverse pressure gradient. At G and H, however, the differences between the two flows are large. To understand this we need an overall

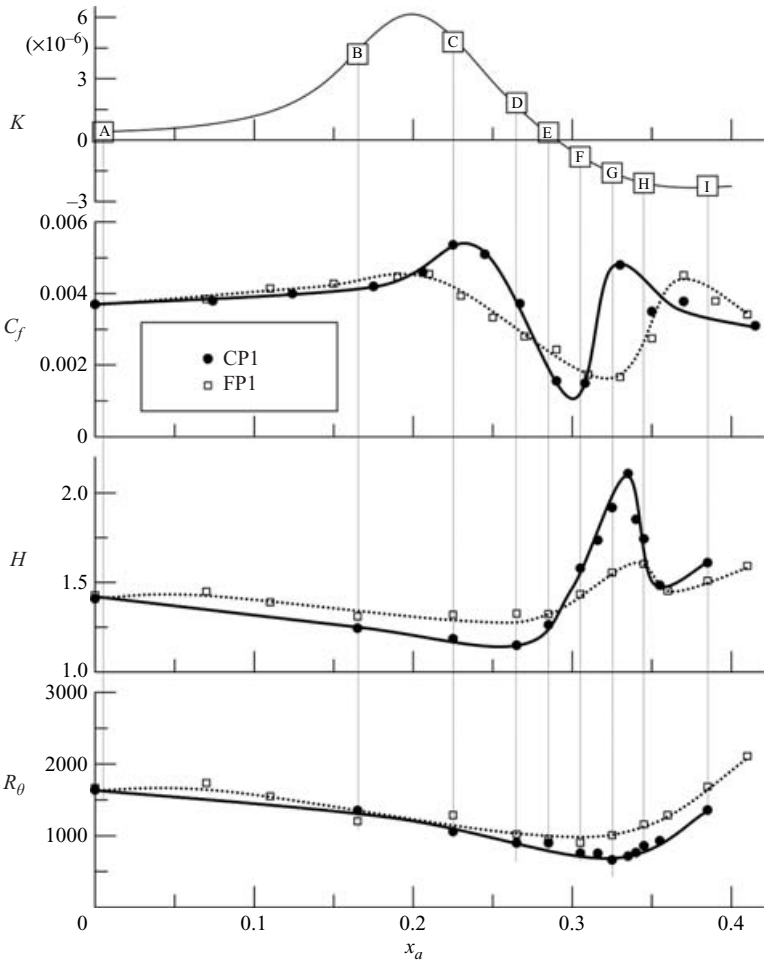

FIGURE 5. A comparison of boundary-layer parameters for flows FP1 and CP1.

appreciation of the complex interactions between pressure gradient and curvature in these flows. This can be achieved by examining boundary-layer parameters such as the skin friction coefficient C_f, the shape factor H and the Reynolds number R_θ.

3.2. *Mean-flow parameters*

The streamwise variations of K, C_f, H and R_θ for both CP1 and FP1 are shown in figure 5. In general the variations are typical of highly accelerated turbulent boundary layers undergoing relaminarization and retransition (e.g. Badri Narayanan & Ramjee 1969; Blackwelder & Kovasznay 1972). The skin friction coefficient C_f initially increases in response to the favourable pressure gradient. As the pressure gradient increases, C_f reaches a peak and progressively decreases to relatively low values indicating relaminarization. It may be noticed that in a small region (of length about 1.5δ) at the beginning of the adverse pressure gradient beyond station E in FP1, C_f is nearly constant, indicating that retransition has not followed immediately. A plausible reason for this slightly delayed retransition is the relatively low inner-viscous-layer Reynolds number in the present flows (estimated to be in the range

150–170, Mukund 2002*b*). As the pressure gradient becomes adverse at some distance beyond station E, C_f rapidly increases indicating retransition. The decrease beyond the second peak is characteristic of the approach to fully turbulent flow following transition, but is partly also the effect of the adverse pressure gradient on the re-formed turbulent boundary layer, which is noticeable in the increase in shape factor beyond station H.

The variation of shape factor H is consistent with that of C_f. It starts decreasing from its initial value of about 1.45 in both CP1 and FP1 as a consequence of the favourable pressure gradient, and continues to do so in the early stages of relaminarization. It starts increasing in CP1 between stations D and E till G/H, reaching a peak value of about 2.2. It then decreases sharply due to retransition, and increases again. The large rise in H for CP1 in the retransition zone (figure 5) is possibly due to the flow near the wall undergoing retransition (as inferred by the increase in C_f), while the outer part of the boundary layer responds to the adverse pressure gradient without being affected by the onset of retransition. A similar but less pronounced feature may be observed in FP1 as well.

The four zones discussed above – namely, the fully turbulent boundary layer in a favourable pressure gradient, the relaminarization zone, the retransition zone, and the re-formed turbulent boundary layer in an adverse pressure gradient – constitute a complete cycle, and can easily be recognized in the C_f plot in figure 5.

The most interesting aspect of figure 5 concerns the differences between CP1 and FP1. Measured C_f and H variations are consistent in indicating that relaminarization and re-transition are both more rapid in CP1 than in FP1. Maximum and minimum values of both C_f and H in CP1 go beyond those in FP1, suggesting that relaminarization in CP1 is more complete. Re-transition also occurs earlier (before station F CP1, around station G FP1). The decrease in H and C_f after their retransition peaks (at station G in CP1, at or beyond station H in FP1) is also more pronounced in CP1 than in FP1. Overall, curvature hastens the occurrence and intensity of relaminarization and retransition, in spite of the slightly later occurrence of maximum C_f and minimum H in CP1 compared to FP1(see figure 10). Finally, figure 5 shows that the minimum value of R_θ attained in CP1 is less than in FP1, consistent once again with the higher degree of relaminarization in the former.

The slower, milder changes in FP1, in spite of the relatively high pressure gradient, raise the question of whether they can be attributed to the relatively short extent of the acceleration – in contrast with earlier work on flat plates.

3.3. *Streamwise turbulence intensity profiles*

An examination of the streamwise turbulent-velocity fluctuations provides additional insight into the role of surface curvature in relaminarization. Figure 6 shows selected time traces of the velocity fluctuations in the near-wall region ($y = 0.6$ mm) for both FP1 and CP1. The fluctuation at the initial station A is typical of a turbulent boundary layer. As the flow accelerates, a progressive quenching of turbulence typical of relaminarizing boundary layers is observed, with the intensity reaching a minimum at station D – values for CP1 being lower than in FP1. At E the amplitude starts increasing due to retransition. At station H the intensities are higher in FP1 than in CP1. This is because H is in the middle of retransition in FP1, whereas it is at the end of the retransition zone in CP1; it is well known that velocity fluctuations reach maximum values within the transition zone (e.g. Schubauer & Klebanoff 1955).

Figure 7 shows the profiles of the normalized streamwise turbulence intensity at various stations, with the flat-plate results of Klebanoff (1955) plotted as reference.

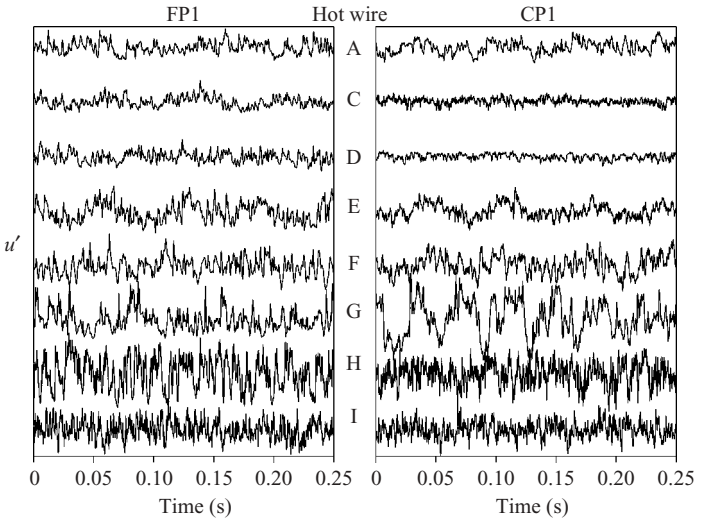

FIGURE 6. Time trace of velocity fluctuations, comparing FP1 and CP1.

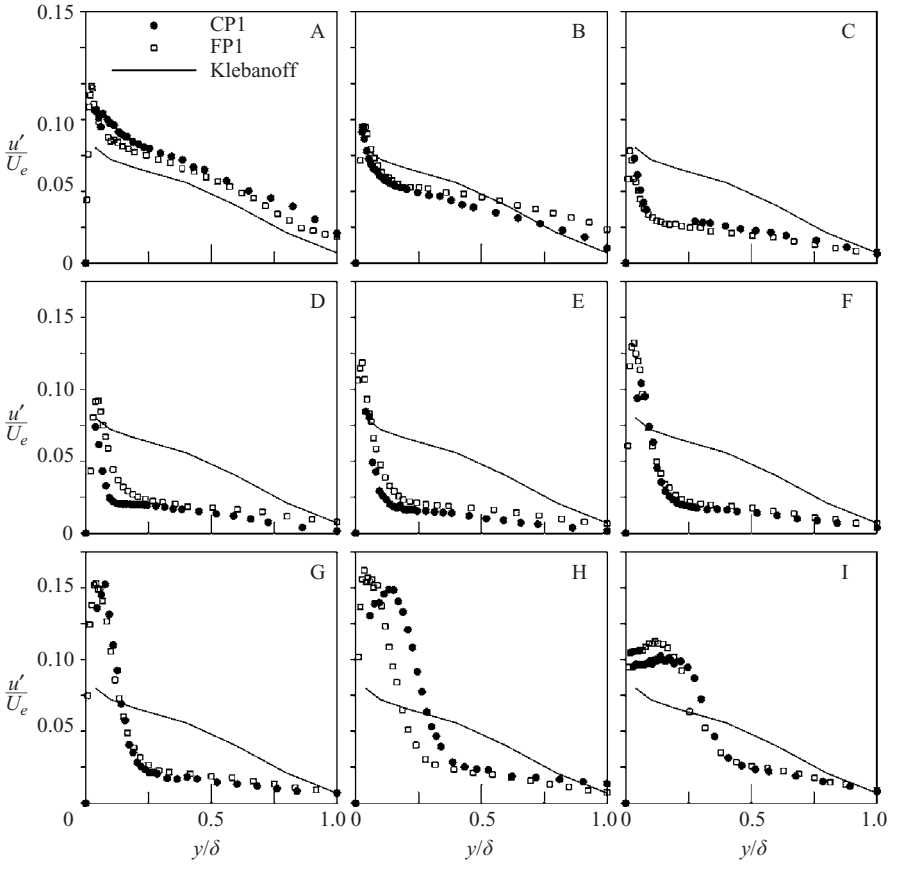

FIGURE 7. Streamwise turbulence intensity profiles.

At station A, where the pressure gradient is still very mild, the profiles are close to the reference profile. Beginning with station B, the turbulence intensities in the outer 90% of the boundary layer reduce rapidly, in a way typical of relaminarization by acceleration. At stations D, E and F the normalized intensities are lower for CP1 than for FP1, consistent with the more rapid relaminarization in CP1. Since turbulence intensities also decrease in convex-surface boundary layers, curvature and pressure gradient are reinforcing each other at these stations in CP1.

Note that, beginning at D, turbulence intensity increases in the inner region and is only weakly affected outside. The peak near the wall moves progressively outwards as the pressure gradient is relieved. The magnitude of the peak reaches a maximum at stations G and H, where the boundary layer is undergoing retransition in an adverse pressure gradient. Further downstream at station I, as the boundary layer becomes fully turbulent (still in an adverse pressure gradient), the peak value decreases with distance and its location moves out in the boundary layer, as may be expected for the general scenario presented here.

The decreasing value of the peak in turbulence intensity is not normally expected in a turbulent boundary layer in an adverse pressure gradient. Since relaminarization essentially involves two layers in the NS73 description, namely the inner viscous and the outer rotational inviscid layers, the entire boundary layer does not respond at the same rate. Thus, the inner layer may undergo retransition, whereas the outer layer, aided by convex curvature with its tendency to suppress turbulence, responds more slowly to the retransition process. However, at station I (and beyond – not shown here), the behaviour is typical of a turbulent boundary layer in an adverse pressure gradient, with higher intensities all across the boundary layer and a peak value that has moved outwards.

Compared to FP1, the streamwise turbulence intensity profiles of CP1 in the acceleration region are lower at stations D to F, presumably due to the effect of curvature. To facilitate quantitative comparison of the two flows, the streamwise development of the turbulence intensities normalized with the respective values at the beginning of acceleration are plotted in figure 8 for various y/δ. As the flow accelerates the turbulence intensities in CP1 are not only lower but also decreasing at a faster rate than in FP1 at all y/δ. In fact, there is hardly any reduction in the initial stages in FP1. This large reduction must be attributed to the influence of convex curvature in CP1.

Finally we look at the power spectral density (p.s.d.) of the u' signals in figure 9. There is little difference between the two flows at station A. From stations C to F flow CP1 has lower energy, especially at the lower frequencies: the difference is about an order of magnitude at C and D. This is a strong indication of the suppression of the large eddies due to convex curvature. At C and D even the high-frequency part of the spectrum is different between the two flows: the decay with frequency is lower in CP1. At station H, CP1 has greater energy at all frequencies, indicative of nearly complete retransition. At station I flow FP1, with transition nearly complete, shows more energy than CP1, which is fully turbulent.

An interesting observation from these spectra is that curvature in combination with pressure gradient seems to affect the cascade process. Thus at all stations in the relaminarizing region, i.e. stations C to F (note there are no data for CP1 at station B), the spectra in FP1 are always higher than in CP1. Nevertheless, the decay rates at high wavenumbers are generally lower in CP1, indicating that the net transport of turbulent energy from lower to higher wavenumbers is affected by curvature. One possibility is that the loss of energy in the large eddies, noted above, appears as a relatively larger inertial transfer to smaller scales.

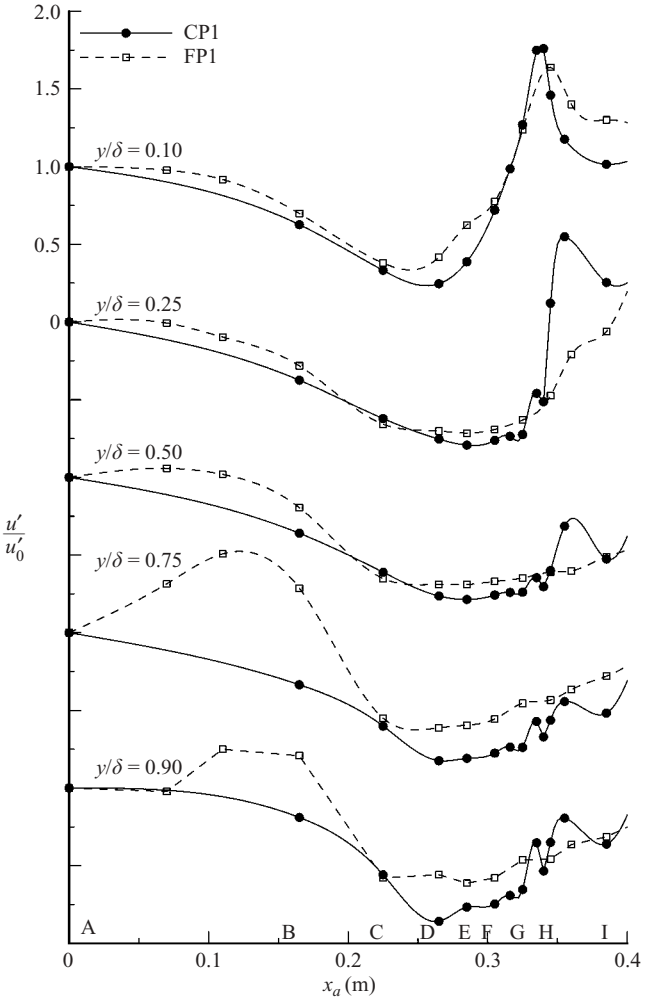

FIGURE 8. Reduction of turbulence with streamwise distance at several locations across the boundary layer ($u_0' = u'$ at $x_a = 0$). Measurement stations A to I are also indicated.

4. Calculations using the quasi-laminar equations

The experimental results discussed above have clearly shown the effect of convex curvature in promoting relaminarization. An attempt is now made to predict the relaminarizing zone in these flows, with focus on seeking further evidence on curvature effects. To the best of our knowledge there are no models that effectively tackle the relaminarization of accelerated turbulent boundary layers on a curved surface (followed by retransition in adverse pressure gradients). We therefore use the quasi-laminar equations (QLE) of NS73, without any modelling for curvature effects, to obtain insight into the dynamics of the flow. This simple approach has the advantage of providing physical explanations for the nature of mean-flow development in the relaminarization zone.

Based on the success of QLE in various relaminarizing flows on flat plates with the acceleration zone extending over distances of order $30\delta_0$, a value of Λ greater than about 50 was suggested for the applicability of the method (NS73). In the present

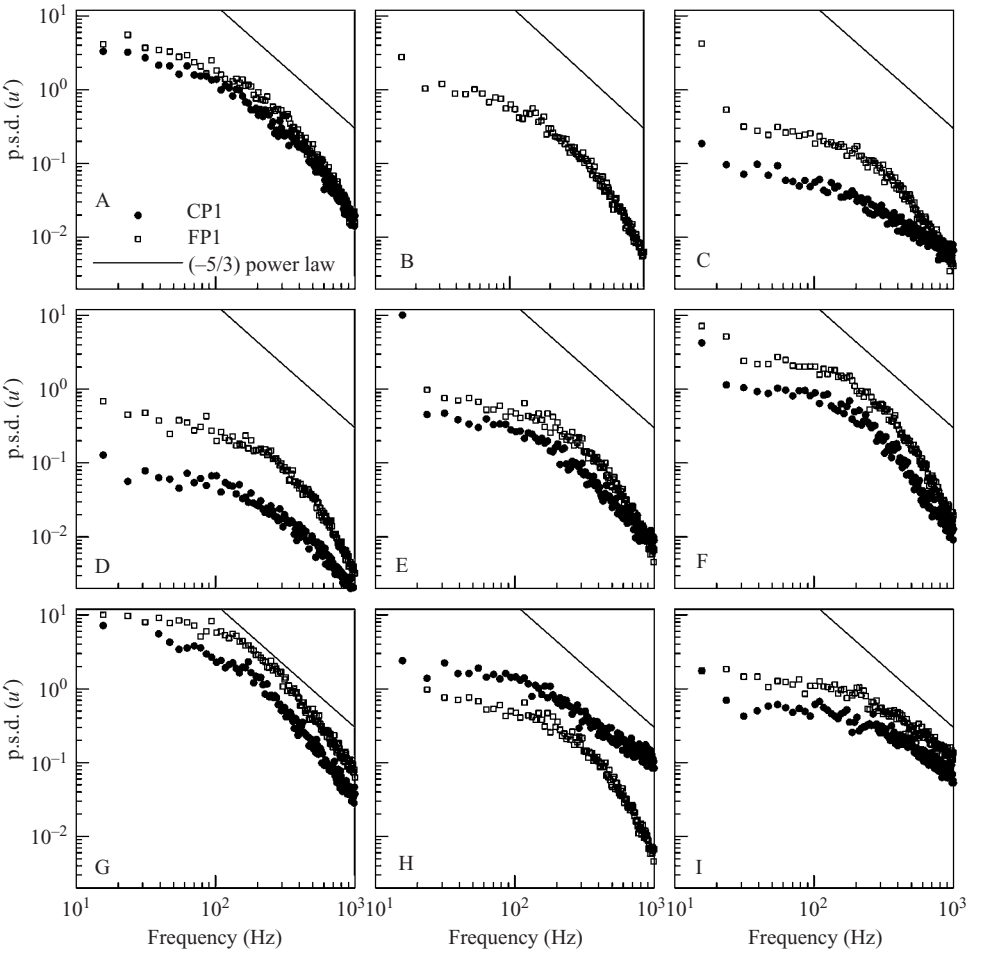

FIGURE 9. Power spectral density of velocity fluctuations.

experiments, the maximum value of Λ is about 158 in both CP1 and FP1 but the extent of acceleration is shorter ($10\delta_0$ to $12\delta_0$ from $K = 0.5 \times 10^{-6}$ to zero through the maximum). The present experiments therefore incidentally provide an opportunity to assess the value of the quasi-laminar approach for gaining insight into relaminarizing flows when the acceleration zone is short and the surface is curved.

In the present calculations the outer inviscid layer is computed using power-law profiles and the inner viscous layer using a variant of the method of Thwaites (1949), with revised values provided by Dey & Narasimha (1990). (This has been necessary because the parameters listed by Thwaites are not entirely satisfactory in highly favourable pressure gradients.) QLE has been successfully validated using data from a large number of relaminarizing boundary layer flows on flat surfaces, including some flows calculated by Sreenivasan (1974). Details of these calculations and comparisons are reported in Mukund (2002*b*).

A comparison of the predictions of C_f using QLE with measured values for the two flows is shown in figure 10. (The differences between predictions for CP1 and FP1 are due to the small differences in the pressure gradient between them.) The prediction for CP1 is in surprisingly good agreement with measurement in the relaminarization

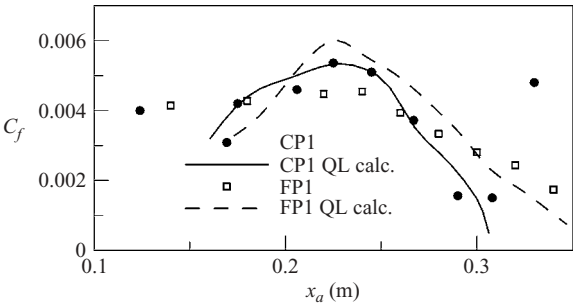

FIGURE 10. Comparing quasi-laminar calculations with experiments for CP1 and FP1.

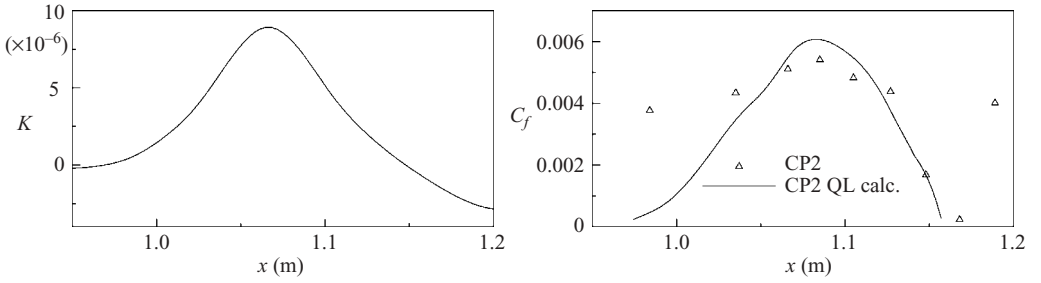

FIGURE 11. Comparing quasi-laminar calculations with experiments for CP2.

zone – from station B to very near station F – despite the fact that the method does not explicitly model curvature effects. Incidentally, the decrease in boundary-layer thickness during relaminarization (by about 50 % in CP1) reduces the value of the local curvature parameter $k\delta$, making it slightly less significant than it might otherwise have been.

The success of QLE may again be seen as applied to flow CP2 (figure 11), which has a $K_{\max}$ of 8.5×10^{-6} and an even shorter zone of acceleration ($7\delta_0$) than CP1. The excellent agreement in both cases (figures 10 and 11) suggests that the convex-surface flows CP1 and CP2 have relaminarized earlier and more completely. This success suggests that the approximations made in deriving QLE are even better satisfied on convex- than on flat-surface flows. This must be due to the faster and stronger response of the outer layer of the boundary layer to curvature effects in CP1, leading to an earlier freezing, and even suppression, of the Reynolds shear stress. Curvature effects in the viscous layer are anyway negligible as they constitute only a second-order effect on a laminar boundary layer (Narasimha & Ojha 1967), and the value of $k\delta_v$ (where δ_v is the viscous layer thickness) is generally only a fraction of $k\delta$. Further, the 'islands of ignorance' (NS73) and the 'laminarescent' regions of Sreenivasan (1982) are shortened in these curved boundary layer flows, once again reflecting the promoting effect of convex curvature on relaminarization. These predictions also add weight to the NS73 hypothesis that, as opposed to the onset of relaminarization and the mechanisms influencing it, the relaminarizing process can be defined and described with much greater confidence.

In contrast, the predictions for FP1 are quantitatively less striking; in particular the predicted fall in C_f in the relaminarization zone is much steeper compared to the experimental data. The inability of QLE to better predict FP1, even when the

maximum value of Λ is significantly higher than 50, is perhaps due to the short extent of the acceleration zone – shorter than in any relaminarizing flow on a flat plate tested to-date.

5. Conclusions

A closely matched pair of convex-surface and flat-plate flows, subjected to virtually identical highly favourable pressure gradients, have been used to study the role of surface curvature in relaminarization. The length of the acceleration zone (normalized by the initial boundary-layer thickness) is significantly shorter than in earlier two-dimensional boundary-layer studies, but is consistent with values that prevail in wing leading-edge flows.

The experimental results yield clear evidence of relaminarization in both flows, but the phenomenon is more marked on the convex surface. In relation to the flat-plate flow FP1, the convex-surface flow CP1 shows a more rapid reduction in skin friction coefficient during relaminarization, a higher maximum value for the shape factor, a lower minimum value for the momentum-thickness Reynolds number, a larger reduction of the relative turbulence intensity throughout the boundary layer, and finally, greater and more rapid reduction of the turbulence energy at lower frequencies in the near-wall region. All these differences show a higher degree of relaminarization due to the presence of convex curvature.

The success of calculations of mean-flow parameters using quasi-laminar equations on the convex surface suggests that the approximations made in deriving the equations are better satisfied on convex-surface flows than on a flat plate. This is because the outer layer of the curved-surface boundary layer responds quickly to curvature effects, which tend to suppress the Reynolds shear stress (not merely freeze it, as in flat-plate flow). Further, the 'islands of ignorance' in these curved boundary layer flows are shortened, once again reflecting the reinforcing effect of convex curvature on relaminarization.

The results show that convex curvature and favourable pressure gradients combine to make relaminarization more rapid as well as complete; thus the simple two-layer theory devised for flat-plate flows works even better for predicting mean flow without having to take explicit account of curvature. This suggests that surface-curvature effects can offset a reduction in the acceleration-zone length. It is also likely that values of pressure gradient parameters like K and Λ required for relaminarization are lowered in the presence of convex curvature, thus enhancing the chances of occurrence of the relaminarization–retransition cycle in the leading-edge region of a swept wing with a turbulent attachment line.

While the focus in the present experiments has been the role of convex surface curvature in the process of relaminarization under severe acceleration, the three flows (FP1, CP1 and CP2) have demonstrated for the first time that relaminarization is indeed possible in considerably shortened zones of acceleration ($7\delta_0$–$12\delta_0$) in comparison with flows investigated in literature with much larger extent of acceleration ($25\delta_0$–$40\delta_0$); undoubtedly, these test cases will pose a significant challenge to modelling and in developing prediction methods. (The experimental data will shortly be available on the website www.nal.res.in/relamdata, and are in Mukund & Viswanath 2006.)

A part of this research was funded by Boeing Commercial Airplanes, USA, which we gratefully acknowledge. R. N. thanks DRDO for support of his research at JNCASR.

REFERENCES

Arnal, D. & Juillen, J. C. 1990 Leading edge contamination and relaminarization on a swept wing at incidence. In *Proc. Numerical and Physical Aspects of Aerodynamic Flows IV* Springer (ed. T. Cebeci), pp. 391–402.

Badri Narayanan, M. A. & Ramjee, V. 1969 On the criteria for reverse transition in a two-dimensional boundary layer. *J. Fluid Mech.* **35**, 225–241.

Blackwelder, R. F. & Kovasznay, L. S. G. 1972 Large-scale motion of a turbulent boundary layer during relaminarization. *J. Fluid Mech.* **53**, 61–83.

Bourassa, C., Thomas, F. O. & Nelson, R. C. 2000 Experimental investigation of turbulent boundary layer relaminarization with application to high-lift systems: preliminary results. *AIAA Paper* 2000-4017.

Bradshaw, P. 1973 Effects of streamline curvature on turbulent flow. *AGARDograph.* 169.

Brandt, R. 1993 Relaminarized boundary layers subjected to adverse pressure gradients. PhD thesis, Engineering Department, Cambridge University; Report CUED/A-Aero/TR-21.

Dey, J. & Narasimha, R. 1990 An extension of Thwaites method for calculation of incompressible laminar boundary layers. *J. Indian Inst. Sci.* **70**, 1–11.

Escudier, M. P., Abdel-Hameed, A., Johnson, M. W. & Sutcliffe, C. J. 1998 Laminarization and re-transition of a turbulent boundary layer subjected to favourable pressure gradient. *Exps. Fluids* **25**, 491–502.

Gibson, M. M., Verriopoulos, C. A. & Vlachos, N. 1984 Turbulent boundary layer on a mildly curved convex surface, 1:mean flow and turbulence measurements. *Exps. Fluids* **2**, 17–24.

Ichimiya, M., Nakamura, I. & Yamashita, S. 1998 Properties of relaminarizing turbulent boundary layer under a favorable pressure gradient. *Expl Thermal Fluid Sci.* **11**, 37–48.

Klebanoff, P. S. 1955 Characteristics of turbulence in a boundary layer with zero pressure gradient. *NACA Rep.* TR 1247.

Kline, S. J. & McClintock, F. A. 1953 Describing uncertainties in single-sample experiments. *Mech. Engng* **1**, 3–8.

Kobashi, Y. & Hayakava, M. 2002 Relaminarization mechanism of turbulent boundary layer in accelerated flow. *Proc. Ninth Asian Congress of Fluid Mechanics, Isfahan, Iran*, pp. 1–6.

Launder, B. E. 1964 Laminarization of the turbulent boundary layer in a severe acceleration. *J. Appl. Mech.* **31**, 707–708.

Launder, B. E. & Loizou, P. A. 1992 Laminarization of three-dimensional accelerating boundary layers in a curved rectangular-sectioned duct. *Intl J. Heat Fluid Flow* **13**, 124–131.

Liepmann, H. W. & Skinner, G. T. 1954 Shearing stress measurements by use of a heated element. *NACA Tech. Note* 3268.

Mukund, R. 2002*a* Relaminarization in a short acceleration zone on a convex surface. PhD thesis, Dept. Aerospace Engineering, Indian Institute of Science, Bangalore; PD EA 0511, National Aerospace Laboratories, Bangalore, 2005.

Mukund, R. 2002*b* Calculation of relaminarizing flow using quasi-laminar equations. PD EA 0202, National Aerospace Laboratories, Bangalore.

Mukund, R. & Viswanath, P. R. 2006 Experimental data on relaminarizing boundary layers on convex and flat surfaces. PD EA 0606, National Aerospace Laboratories, Bangalore.

Narasimha, R. & Ojha, S. K. 1967 Effect of longitudinal surface curvature on boundary layers. *J. Fluid Mech.* **29**, 187–199.

Narasimha, R. & Sreenivasan, K. R. 1973 Relaminarization in highly accelerated turbulent boundary layers. *J. Fluid Mech.* **61**, 417–447 (referred to herein as NS73).

Narasimha, R. & Sreenivasan, K. R. 1979 Relaminarization of fluid flows. *Adv. Appl. Mech.* **19**, 221–309.

Patel, V. C. & Sotiropoulos, F. 1997 Longitudinal curvature effects in turbulent boundary layers. *Prog. Aero. Sci.* **33**, P1–70.

Prabhu, A., Narasimha, R. & Rao, B. N. S. 1983 Structure and mean-flow similarity in curved turbulent boundary layers. In *Proc. IUTAM Symposium on Structure of Complex Turbulent Shear Flow* (ed. R. Dumas & L. Fulachier), pp. 100–111. Springer.

Prabhu, A. & Sundarasiva Rao, B. N. 1981 Turbulent boundary layers in a longitudinally curved stream. *Rep.* 81 FM 10, Dept. Aero. Engng, Indian Inst. of Science, Bangalore.

Schubauer, G. B. & Klebanoff, P. S. 1955 Contributions on the mechanics of boundary layer transition. *NACA TN* 3489.

Schwarz, A. C. & Plesniak, M. W. 1996 Convex turbulent boundary layers with zero and favorable pressure gradients. *Trans. ASME: J. Fluids Engng* **118**, 787–794.

So, R. M. C. & Mellor, G. L. 1973 Experiment on convex curvature effects in turbulent boundary layers. *J. Fluid Mech.* **60**, 43–62.

Sreenivasan, K. R. 1974 Mechanism of reversion in highly accelerated turbulent boundary layers. PhD thesis, Dept Aero. Engng, Indian Inst. of Science, Bangalore.

Sreenivasan, K. R. 1982 Laminarescent, relaminarizing and retransitional flows. *Acta Mechanica.* **44**, 1–48.

Thompson, B. G. J. 1973 The prediction of boundary-layer behaviour and profile drag of infinite yawed wings. *RAE Tech Rep.* 73091.

Thwaites, B. 1949 Approximate calculation of the laminar boundary layer. *Aero. Q.* **1**, 245–280.

Van Dam, C. P., Viggen, P. M. H. W., Yip, L. P. & Potter, R. C. 1993 Leading-edge transition and relaminarization phenomena on a subsonic high lift-system. *AIAA Paper* 93-3140.

Viswanath, P. R., Mukund, R., Narasimha, R. & Crouch, J. D. 2004 Relaminarization on swept leading edges under high-lift conditions. *AIAA Paper* 2004-99.

Warnack, D. & Fernholz, H. H. 1998 The effects of a favorable pressure gradient and of the Reynolds number on an incompressible axisymmetric turbulent boundary layer. Part 2. The boundary layer with relaminarization. *J. Fluid Mech.* **359**, 357–381.

Yip, L. P., Viggen, P. M. H. W., Hardin, J. D. & Van Dam, C. P. 1993 In-flight pressure distributions and skin friction measurements on a subsonic transport high-lift wing section. AGARD, CP-515.